Journal of Organometallic Chemistry 896 (2019) 59–69

Contents lists available at ScienceDirect

Journal of Organometallic Chemistry

journal homepage: www.elsevier.com/locate/jorganchem

Synthesis and characterization of a new poly α-amino acid Co(II)-complex supported on magnetite graphene oxide as an efficient heterogeneous magnetically recyclable catalyst for efficient free-coreductant gram-scale epoxidation of olefins with molecular oxygen

Milad Kazemnejadi [a, *], Boshra Mahmoudi [b], Zeinab Sharafi [c], Mohammad Ali Nasseri [a], Ali Allahresani [a], Mohsen Esmaeilpour [d]

[a] Department of Chemistry, Faculty of Sciences, University of Birjand, Birjand, 97175-615, Iran
[b] Research Center, Sulaimani Polytechnic University, Sulaimani, 46001, Kurdistan Region, Iraq
[c] Razi Herbal Medicines Research Center, Lorestan University of Medical Sciences, Khorramabad, Iran
[d] Department of Chemistry, College of Science, Shiraz University, Shiraz, 7194684795, Iran

ARTICLE INFO

Article history:
Received 18 April 2019
Received in revised form
28 May 2019
Accepted 31 May 2019
Available online 3 June 2019

Keywords:
Graphene oxide
Epoxidation
Fe_3O_4
Nanocatalyst
Magnetically recyclable
Gram-scale

ABSTRACT

A novel magnetic nanocomposite was prepared by immobilization of a cobalt complex of a synthetic poly α-amino acid on Fe_3O_4-doped graphene oxide (GO/Fe_3O_4@PAA Co(II)) and was demonstrated to be a highly efficient catalyst for the epoxidation of olefins in mild conditions. PAA was synthesized through a multi-step synthesis, first by a poly condensation reaction of salicylaldehyde followed by the Strecker synthesis. The synthesized nanocomposite was characterized by various analytical and spectroscopic methods including FTIR, ICP, XRD, EDX, XPS, FE-SEM, TEM, TGA, VSM and DLS analyses. A wide variety of olefins could be tolerated toward epoxidation in the presence of molecular oxygen without the need for any co-reductant. The magnetic nanocomposite could be readily separated by a magnet from the mixture and reused for several times without any significant reactivity loss, which represents its potential for practical and industrial application. Also, the scalability of the process was investigated in this work.

1. Introduction

Epoxides are one of the key and versatile intermediates for manufacture of fine chemicals including plasticizer, perfumes, cosmetics, epoxy resins, pharmaceuticals, etc. [1]. Traditionally, epoxides are synthesized by stoichiometric amount of oxidizing reagent such as potassium monoperoxysulfate [2] and organic peracids [3]. These peroxides are not only toxic, corrosive and harmful, but also generate toxic waste products, which limited their application in industrial aspects as well as in laboratory due to the safety issues. So, the researches were conducted to use more convenient, easily handling and environmentally friendly oxidants such as molecular oxygen, TBHP, air and hydrogen peroxide [3,4]. In order to exploit the advantage of these oxidants for epoxidation, as the easily accessible and green oxidants, there is a need for a transition metal in order to oxygen transfer [5]. Various catalytic systems based on transition metals have been developed recently such as: (1) Fe_2/mpg-C_3N_4 (mesoporous carbon nitride) [6], (2) mesoporous cobalt oxide [7], (3) zeolites [8], (4) nickel complexes [9], (5) Mn(II) and (III) complexes [10], (6) Mn-porphyrin [11], (7) Cu_2(oxalate)(1,10-phen)$_2Cl_2$ [12], (8) [Mo(η^3-C_3H_5)Br(CO)$_2${^{i}PrN = C(H)C_5H_4N}] [13], and (9) Rh_2(tpa)$_4$ (tpa = triphenylacetate) [14].

Despite various progress in this topic, however, most of the reported methods are involve expensive reagents, unsatisfactory yield, low selectivity, non-environmentally benign, using co-reductant, harsh reaction conditions, etc. It worth noted that two excess possible products could be obtained in result of the epoxidation of an olefins bearing Hα (Scheme 1) [15], which is not

* Corresponding author.
E-mail address: miladkazemnejadi@birjand.ac.ir (M. Kazemnejadi).

https://doi.org/10.1016/j.jorganchem.2019.05.030
0022-328X/

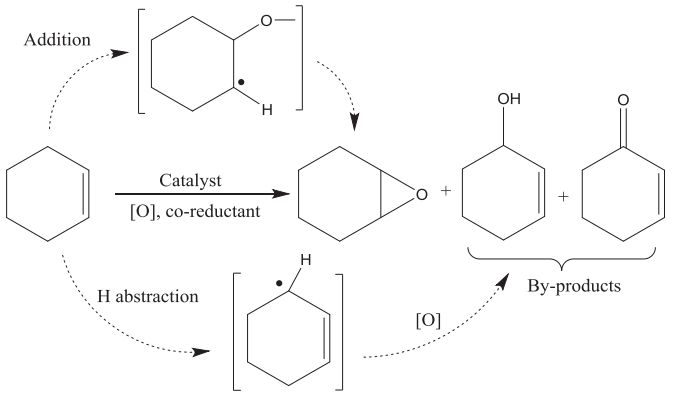

Scheme 1. Epoxidation of cyclohexene catalyzed by the transition metal catalytic systems.

suitable for practical aspects. So, finding a highly efficient catalytic system with high selectivity and toxicity, which involves green chemistry considerations seems essential.

Application of nanomaterials as a solid support due to their high ratio of surface to volume are well known for decades [16,17]. Among them, graphene oxide (GO) with the interesting properties such as sheet structure, nano-size dimension with high surface area, high thermal/chemical stability and possibility of functionalization with various organic compounds become as one of the most suitable solid supports for organic synthesis [3,4,18]. Further improvement in heterogeneous catalysts led to the preparation of magnetic nanoparticles that facilitates the separation of catalyst with an external magnetic field [19]. Fe_3O_4 nanoparticles are one of the most applicable and popular magnetic nanoparticles due to their widespread applications in various fields of area such as catalyst and medicine [5,20]. Some advantages are associated with them including low cost, high thermal stability, non-toxic, chemical stability, strong magnetization, and high crystalline structure, which conducted them for magnetization of other solid supports; this is a smart strategy for magnetization of solid supports (in this case nano graphene oxide), which has been used extensively in the last decades [3,19].

Cobalt complexes and generally Co-based catalytic systems have received attention due to their well-known potential for oxidation programs, being cheap and accessible, and non-toxic nature [21]. Herein, in accordance with green chemistry considerations and also importance and application of useful epoxides in organic synthesis, we plan a multiphase nanocomposite with decoration of a Co(II) complex of a synthetic poly α-amino acid onto magnetic graphene oxide as an highly active heterogeneous magnetically recoverable catalyst for the efficient free-coreductant gram-scale O_2-epoxidation of olefins in mild conditions. This system not only benefits from advantages of a solid nano-support with high aspect ratio (graphene oxide), but also utilizes from the presence of PAA as a strong ligand on its surface that is responsible for high durability and activity of the catalyst.

2. Experimental

2.1. Materials and apparatus

All chemicals were obtained from Sigma and Fluca supplier and used as received without further purification. All the solvents were distilled and dried before use. Progress of the reactions and purity of products were monitored by thin layer chromatography (TLC) on silica gel and/or gas chromatography (GC) on a Shimadzu-14B gas chromatography equipped with HP-1 capillary column and N_2 as carrier gas. For GC analyses, anisole was used as an internal standard. Purification of imines and oximes was achieved by recrystallization from ethanol. FTIR spectra were obtained using a JASCO FT/IR 4600 spectrophotometer using KBr pellet. The ^{1}H NMR (250 MHz) and ^{13}CNMR (62.9 MHz) spectra were recorded on a Bruker Avance DPX-250 spectrometer in $CDCl_3$ and DMSO-d_6 as solvent. Transmission electron microscopy (TEM) images were taken on a Philips EM208 microscope and was operated at 100 kV. The presence of the elements was detected by EDX spectroscopy using field emission scanning electron microscope (FE-SEM, JEOL 7600F), equipped with a spectrometer of energy dispersion of X-ray from Oxford instruments. Size distribution of the nanoparticles were measured by dynamic light scattering (DLS) analysis on a HORIBA-LB550 instrument. TGA of the samples have been performed on a NETZSCH STA 409 PC/PG in nitrogen atmosphere with a heating rate of 10 °C/min in the temperature ranges of 25–1000 °C. The magnetic behavior of the samples was conducted on Lake Shore vibrating sample magnetometer (VSM) at room temperature. ICP experiments were accomplished using VARIAN VISTA-PRO CCD simultaneous ICP-OES instrument. Conversion and epoxide selectivity was measured according to the following equations (1) and (2) [1,5]:

$$\text{conversion (mol\%)} = \frac{(\text{initial mol\%}) - (\text{final mol\%})}{\text{initial mol\%}} \times 100 \qquad (1)$$

$$\text{Styrene epoxide selectivity} = \frac{\text{GC peak area of styrene epoxide}}{\text{GC peak area of all products}} \times 100 \qquad (2)$$

2.2. Preparation of PAA

In order to preparation of poly(α-amino acid) (PAA), firstly, poly salicylaldehyde (PSA) was prepared according to a previously reported procedure [1,5,20]. PSA (0.1 g, $\overline{M_n} = 2226$) was added to 20 mL of water, then NaCN (0.5 g, 10 mmol) and NH_4Cl (0.5 g, 10 mmol) were added to the reaction mixture. The reaction was refluxed at 50 °C for 12 h. The resultant orange product (mp > 400 °C, $\overline{M_n} = 2400$), poly(α-amino nitrile) **3**, was isolated by simple filtration followed by drying into oven (50 °C) for 5 h. Poly(α-amino nitrile) was transformed to poly(α-amino acid) by hydrolysis of nitrile groups; 0.2 g of **3** was added to 15 mL of water along with several drops of H_2SO_4, and the mixture was refluxed at 80 °C for 12 h. The mixture reaction was cooled to room temperature and neutralized with 0.5 N KOH solution. Poly(α-amino acid) **4**, was filter off, drying and isolated as a stable powder (mp > 400 °C). Scheme 2 shows the preparation of PAA **4** *via* a multistep synthesis.

2.3. Preparation of GO

Graphene oxide (GO) was prepared according to a modified Hummer's method from purified natural graphite [22,23].

2.4. Preparation of GO/Fe_3O_4 hybrids

GO–Fe_3O_4 hybrid was prepared *via* a chemical co-precipitation method according to the slightly modified literature procedure [24,25]. GO/Fe_3O_4 NPs were prepared with a mass ratio of 1: 5 (GO: $FeSO_4$). This premium ratio provides a suitable responsive to a magnetic field for the readily separation of the NPs [4]. In a typical

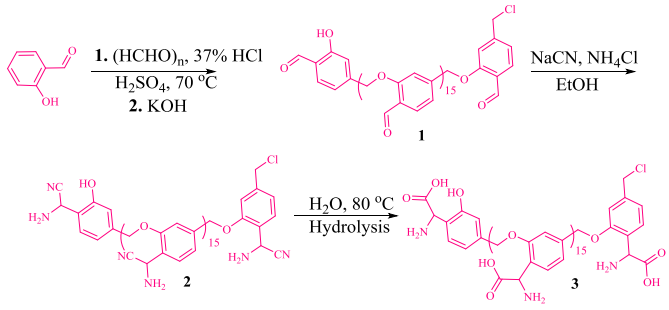

Scheme 2. Synthesis of poly(AA).

process, GO (25 mg) was first sonicated in 150 mL deionized water for 10 min. The mixture was stirred and heated to 80 °C in an oil bath. Then, NH_4OH 25% solution was added dropwise to the mentioned solution until the pH adjusted to 11. Then, $FeSO_4.7H_2O$ (125 mg) along with sodium dodecyl sulfate (SDS) were added into the aqueous dispersion of GO solution. The resulting mixture was stirred under N_2 atmosphere for 24 h at 80 °C. The GO/Fe_3O_4 nanoparticles were collected by an external magnetic field followed by washing with deionized water several times in order to eliminate the excess iron salts. Finally, the product was separated by a simple external magnet, then dried in vacuum (40 °C) for 4 h (Scheme 2).

2.5. Preparation of GO/Fe_3O_4@PAA-Co(II) complex

For the preparation of GO/Fe_3O_4@PAA complex, 20 mg of GO/Fe_3O_4 in 50 mL DMF was ultra-sonicated for 1 h, and then 0.2 g of *N,N′*-dicyclohexylcarbodiimide (1.0 mmol, DCC) and 4-dimethylaminopyridine (DMAP) along with 0.5 g of PAA were added into the solution. The resultant mixture was stirred for 8 h at 80 °C under N_2 atmosphere. The product, GO/Fe_3O_4@PAA **7**, was separated using an external magnetic field and washed with water for several times until the pH reached to 7, and then dried into oven (60 °C). Complexation of cobalt to GO/Fe_3O_4@PAA was takes place by sonication of GO/Fe_3O_4@PAA (1.0 g) in 20 mL EtOH followed by addition of $Co(OAc)_2$ (10 mg) to the solution. The mixture was stirred at room temperature for 2 h. The product **8** was purified as same as the previous step using an external magnetic field.

2.6. General procedure for catalytic epoxidation of olefins by GO/Fe_3O_4@PAA-Co(II)

In a typical run, in a three-necked round-bottom flask equipped with a $O_{2\,(g)}$ inlet (bubbling 15 mL/min, 1.0 atm.), a condenser and a magnet stirrer bar, a mixture of styrene (10.0 mmol) and catalyst **8** (50 mg, 0.2 mol%) were stirred in CH_3CN (10 mL) at 60 °C. The reaction progress was monitored by TLC. Upon reaction completion, the catalyst was magnetically filtered, and the residue was directly subjected to GC instrument to quantify the epoxide product. Moreover, the desired epoxide product was purified by column chromatography followed by identification by ^1H NMR and ^{13}C NMR spectra. Activity of the catalyst was expressed by turnover frequency (TOF) as well as turnover number (TON) [1,5].

3. Results and discussion

3.1. Catalyst characterization

According to GPC analysis of the prepared poly(α-amino nitrile), $M_w = 2400$, it could be calculated that the present nitrile functions per mole of poly(α-amino nitrile) is 17/2400 = 7 mmol. So, assuming that all of the nitrile groups are converted to acid; the poly(α-amino acid) contain 7.0 mmol acid functions per gram of PAA.

FTIR spectra of 5-chloromethyl salicylaldehyde, **2**, **3**, **4**, GO (**5**), **6**, **7**, and **8** are shown in Fig. 1. The characteristic peaks at 725 cm^{-1}, 1481 cm^{-1}, and some series vibrations at 2900-2950 cm^{-1} are related to C–Cl (Str.), C–H (Aliphatic, Bend.), and C–H (Aliphatic, Str.) vibrations, respectively, which completely confirmed the chloromethylation of salicylaldehyde (Fig. 1a) [1,5,20]. The polymerization of 5-chloromethyl salicylaldehyde causes to a large reduction of O–H stretching vibration intensity at 3400 cm^{-1}, confirming that the polymerization takes place through the ether bond formation (Fig. 1b) [20]. The preparation of α-amino nitrile *via* the Strecker synthesis was characterized by a strong peak at 2110 cm^{-1} related to CN (nitrile) groups (Fig. 1c). Moreover, two characteristic peaks at 3500 and 3550 cm^{-1} demonstrating the presence of primary amine groups (Stretching vibrations). Elimination of the sharp peak refer to nitrile at the spectrum of **4**, confirmed clearly their transformation to carboxylic acids (Fig. 1d). This reduction along with a red shift of the amine groups in FTIR spectrum of poly(α-amino acid), could be related to the formation of COO^- NH_3^+, that is characteristic for a typical amino acid [26]. Fig. 1e, shows the FTIR spectrum of graphene oxide. A peak at 1735 cm^{-1} was assigned to the stretching vibration of C=O for carboxylic groups (Fig. 1e). The intense bond at 3422 cm^{-1} is attributed to the stretching vibration of hydroxyl groups of GO surface. The peak at 1626 cm^{-1} represents C=C stretching vibrations for aromatic rings related to the non-oxidized graphene oxide framework [27]. Advent of a strong absorption at 572 cm^{-1} at GO/Fe_3O_4 FTIR spectrum indicates the Fe–O (Str.) nanoparticles, confirming the incorporation of Fe_3O_4 NPs on the GO. Another characteristic peak was the reduction of O–H bond intensity due to the decoration of Fe_3O_4 on the graphene oxide (Fig. 1f). Fig. 1g shows the amide bond linkage in **7** at 1622 cm^{-1}. A shoulder at 1635 cm^{-1} could be attributed to free C=O carboxylic bonds. Also, vibrations about 1400 cm^{-1} represents the bending vibration of methylene groups in the polymer (Fig. 1g). Reduction in the intensity of peaks at carboxylic region, confirmed the successful coordination of cobalt cations through these functional groups as indicated in Scheme 3 (Fig. 1h). Furthermore, advent of a series of packs at ~479 cm^{-1} shows the Co–O bond stretching vibration [28], confirming the successful coordination of Co (Scheme 3).

The magnetic property of the samples was studied by VSM analysis. The samples give suitable and satisfactory response to the applied magnetic field (Fig. 2A). No hysteresis phenomenon was found for the samples, which is characteristic for the superparamagnetic nanoparticles [29]. These results confirmed the incorporation of Fe_3O_4 NPs on GO. For comparison, Fe_3O_4 NPs were separately prepared and studied by VSM. The analyses show 78 emu. g^{-1}, 65 emu. g^{-1}, and 32 emu. g^{-1} saturation magnetization for Fe_3O_4, GO/Fe_3O_4, and GO/Fe_3O_4@PAA-Co(II) respectively (Fig. 2A, a-c). The results indicate a large reduction in magnetization for the catalyst **8**, which represent the functionalization of GO in each step (Fig. 2A–c).

The samples were further characterized by TGA analysis. TGA spectrum of GO/Fe_3O_4 indicates three main weight losses (Fig. 2B–a). In the first stage, a slow weight loss takes place near 80 °C correspond to 9% weight loss due to desorption of water [18]. Another weigh loss occurs around 220° with a mild slope, which last to 440 °C. This 18% weight loss exhibited the vaporization and decomposition of various functional groups (Fig. 1a) on GO framework (Fig. 2B–a). Finally, decomposition of $-COO^-$ groups provide 12% weight loss above 600 °C in agreement with the literature [3,18]. An enhancement in thermal stability of GO/

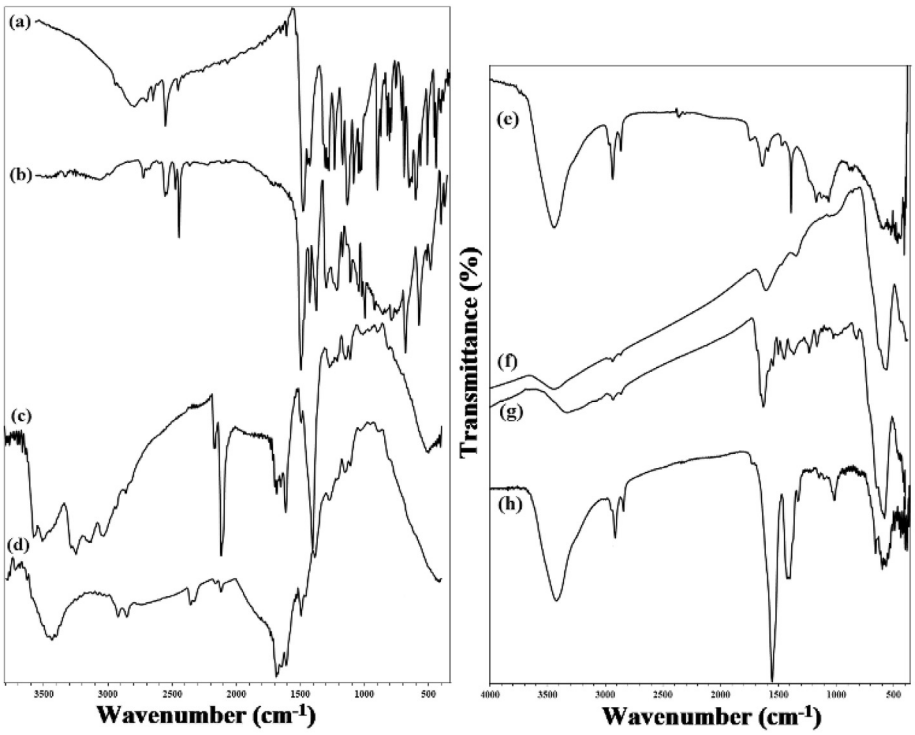

Fig. 1. FTIR spectra of (a) 5-chloromethyl salicylaldehyde, (b) poly salicylaldehyde (**2**), (c) poly(α-amino nitrile) (**3**), (d) poly(α-amino acid) (**4**), (e) GO (**5**), (f) Fe_3O_4/GO (**6**), (g) GO/Fe_3O_4@PAA (**7**), (h) GO/Fe_3O_4@PAA-Co(II) (**8**).

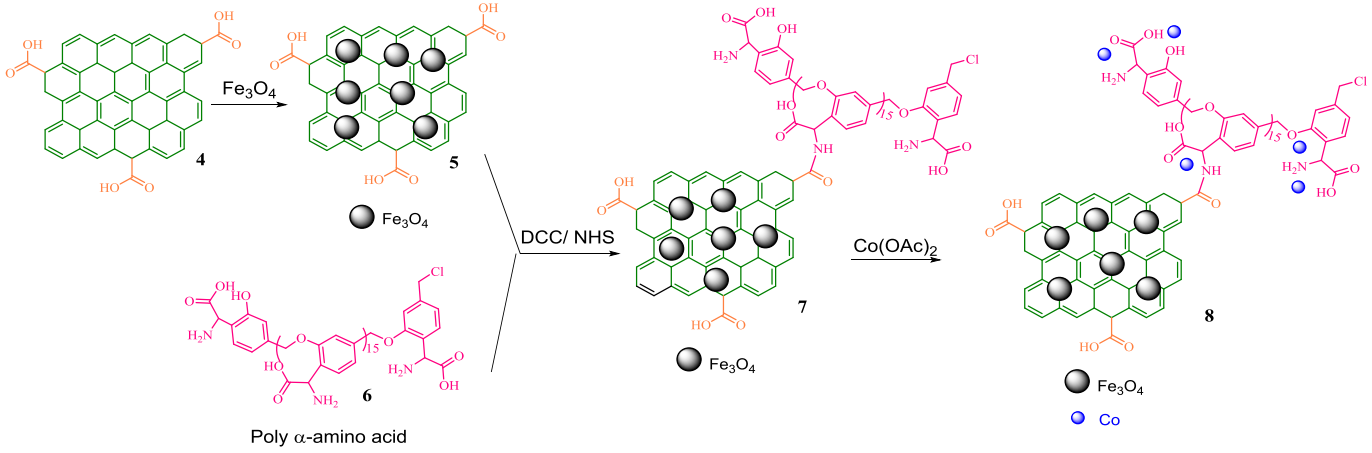

Scheme 3. Synthesis of GO/Fe_3O_4@PAA Co(II) complex.

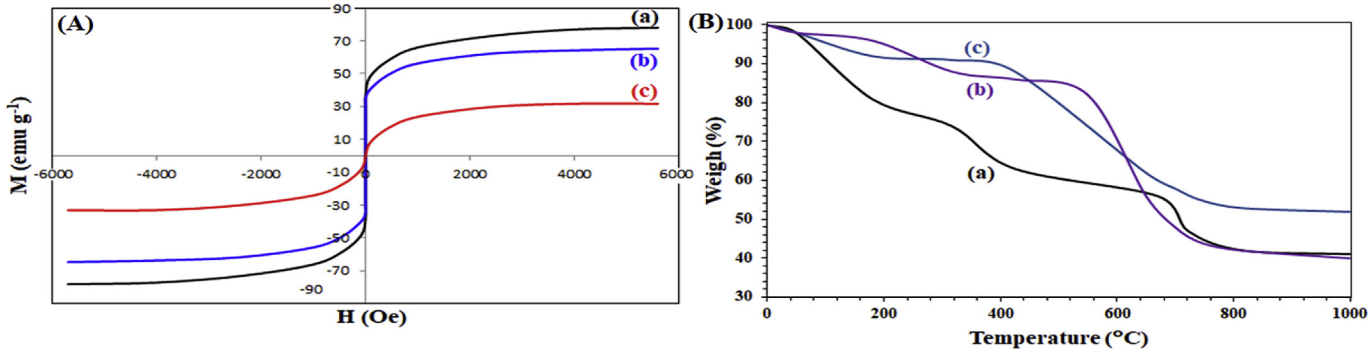

Fig. 2. (A) VSM curves of (a) Fe_3O_4, (b) GO/Fe_3O_4, and (c) GO/Fe_3O_4@PAA-Co(II). (B) TGA spectra of (a) GO/Fe_3O_4, (b) GO/Fe_3O_4@PAA and (c) GO/Fe_3O_4@PAA-Co(II).

Fe_3O_4@PAA was observed, demonstrating the influence of the coated PAA on GO/Fe_3O_4 hybrid. Again, the small weigh loss is due to the release of water on the GO/Fe_3O_4@PAA at 180 °C (10% weight loss). The main weight loss in temperature range of 550–820 °C represents the decomposition of PAA on the GO/Fe_3O_4 (Fig. 2B–b). This weigh loss is equal to 40% and confirming the loading amount of PAA on the NPs. Coordination of cobalt to GO/Fe_3O_4@PAA-Co(II) showed an enhance in its thermal stability, which the overall weight loss was found to be 52% at 1000 °C (compared to GO/Fe_3O_4@PAA-Co(II) with 57% weight loss). This difference may be attributed to the coordinated cobalt in the GO/Fe_3O_4@PAA-Co(II) (Fig. 2B–c). Also, the peak refer to the decomposition of polymer takes place in lower temperatures with a milder slope, that could be attributed to the effect of coordinated cobalt to PAA.

XRD patterns of GO, GO/Fe_3O_4 and GO/Fe_3O_4@PAA-Co are shown in Fig. 3A. GO presents an amorphous peak at $2\theta = 10.8°$ related to (001) plane, that is characteristic for the graphene oxide [4]. Fig. 3A–a, shows the XRD pattern of GO/Fe_3O_4 with six characteristic peaks at $2\theta = 30.3°$, 35.5°, 43.2°, 53.8°, 57.5°, 62.9°, which were assigned to their indices (220), (311), (440), (442), (511), and (440) respectively [3,4]. These reflections were in agreement with the crystal structure of Fe_3O_4 NPs (JCPDS no. 19–0629). As shown in Fig. 3A–b, the intensity of the peak at 10.8° is largely reduced. This behavior suggests that the Fe^{2+} ions act as a reducing agent for graphene oxide [3,19]. The crystal structure of the catalyst **8**, was also demonstrated the peaks for Fe_3O_4 crystal structure as well as a new amorphous peak at $2\theta = 11.5°$.This peak could be assigned to the amorphous PAA in comparison with the GO/Fe_3O_4 XRD pattern, that is coated on the GO framework. Furthermore, the results also proved that the functionalization of GO/Fe_3O_4 with PAA doesn't lead to the phase change of Fe_3O_4 NPs.

The presence of elements in the catalyst **8** was detected by EDX analysis. As shown in Fig. 3B, the elements C, O, N, Co, and Fe were detected, which confirming the structure of **8**. The high resolution XPS Co2p spectrum of GO/Fe_3O_4@PAA-Co(II) revealed the oxidation state of Co (II) ions in the catalyst. As shown in Fig. 3C, the $Co2p_{1/2}$ and $Co2p_{3/2}$ lines were appeared at 797.2 eV and 781 eV respectively, which confirms that Co(II) is the only component in GO/Fe_3O_4@PAA-Co(II) and all Co ions are in +2 oxidation state.

The amount of cobalt in GO/Fe_3O_4@PAA-Co(II) was also determined by ICP analysis which is 0.40 mmol g^{-1}. This amount was completely in agreement and consistence with the results from TGA analyses (Fig. 2B–c).

The morphology of the NPs was studied by FE-SEM technique. As shown in Fig. 4a and b, the images clearly demonstrated the chemical deposition of Fe_3O_4 NPs on GO framework. The results from TEM analysis, also, confirmed the preparation of GO/Fe_3O_4@PAA-Co(II) hybrid with an average size of 28 nm for the particles (Fig. 4c). The results obtained from DLS analysis (Fig. 4d), revealed that the main size distribution of the NPs are in the range of 25–30 nm. The mean size of the NPs was found to be 30 nm with a deviation of 8.2, in agreement with the corresponding TEM image.

3.2. Optimization of reaction parameters

To explore the catalytic activity of GO/Fe_3O_4@PAA-Co(II), the epoxidation reaction of olefins was conducted in the presence of GO/Fe_3O_4@PAA-Co(II). First, for optimization of the reaction conditions, effective parameters involve in the reaction such as temperature, solvent, oxygen flow rate, and catalyst amount were studied over the epoxidation of styrene as a model reaction. As shown from the spectra in Fig. 5, all mentioned parameter played a crucial role in the epoxidation reaction. Acetonitrile and DMF afforded the most efficiencies among the used solvents with 93%

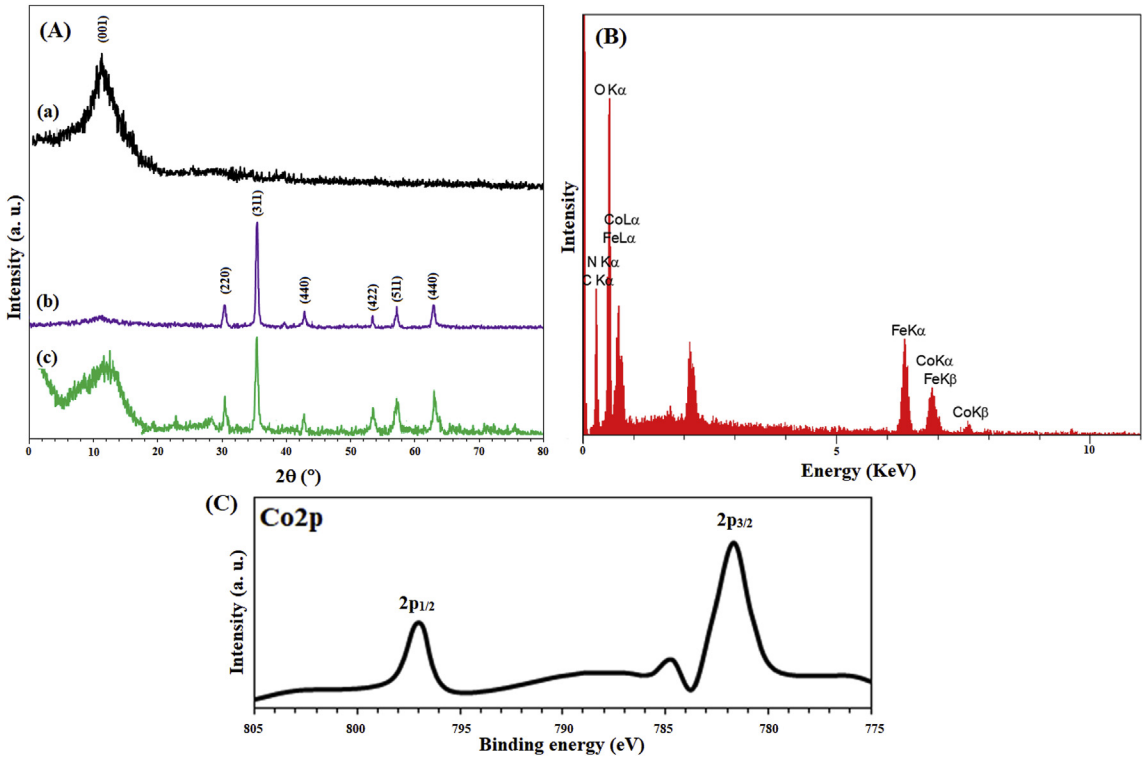

Fig. 3. (A) XRD patterns of (a) GO, (b) GO/Fe_3O_4, (c) GO/Fe_3O_4@PAA-Co. (B) EDX spectrum of GO/Fe_3O_4@PAA-Co (II). (C) High resolution normalized XPS Co2p spectrum of GO/Fe_3O_4@PAA-Co (II).

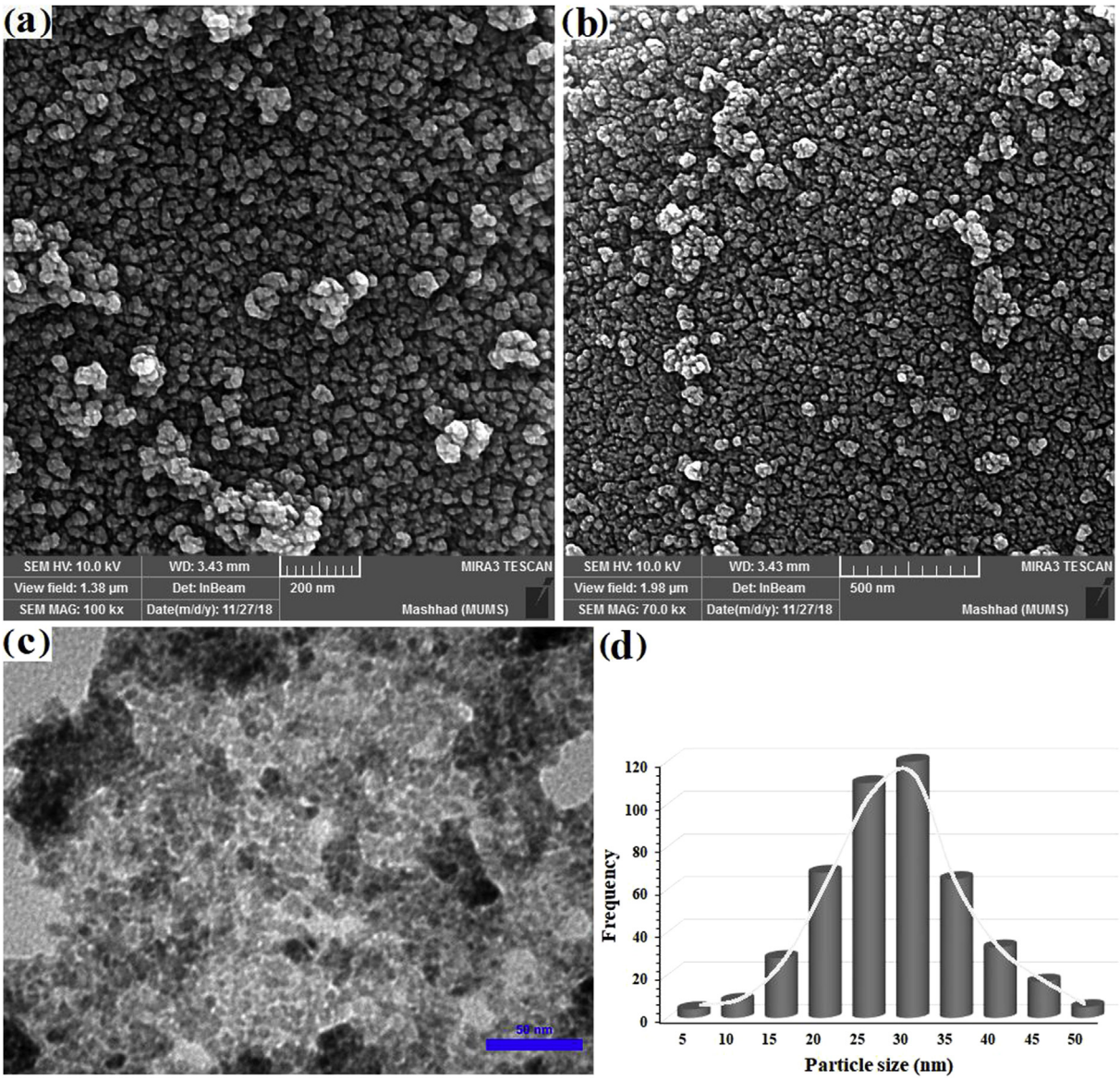

Fig. 4. (a), (b) FE-SEM images, (c) TEM image, and (d) DLS analysis of GO/Fe_3O_4@PAA-Co(II)

conversion (Fig. 5a). It seems that high dielectric constants associated with them ($\varepsilon = 36.46, 38.25$ for CH_3CN and DMF respectively) are responsible for this excellent efficiencies. This property is in agreement with the proposed radical mechanism in the next section involves polar substrates and intermediates. Low conversions for epoxy styrene were obtained in DEE, EtOH, and MeOH. It worth noted that the selectivity is strongly depend on the solvent. The highest selectivity was obtained for EtOH (Figs. 5a and 98%). Then, the model reaction was performed in various amount of the catalyst (Fig. 5b). The most possible efficiency was obtained when the reaction was carried out in the presence of 0.2 mol% of GO/Fe_3O_4@-PAA-Co(II). Didn't found any significant influence on selectivity at other catalyst amounts. Oxygen flow rate of 15 mL/min and 60 °C (CH_3CN) give epoxy styrene with high efficiency (Fig. 5c). The selectivity linearly dropped in higher O_2 concentrations or temperatures. It may be due to promotion of side oxidation products in these conditions.

Catalytic performance of GO/Fe_3O_4@PAA-Co(II) was investigated toward a variety of olefins including aliphatic, conjugated, cyclic, and in other hand, terminal or internal types under obtained premium conditions. The results including time, conversion, epoxide selectivity and TOF were tabulated in Table 1. The method demonstrated high efficiency in terms of TOF and epoxide selectivity for all substrates (Table 1, **10a**-**10m**). Surprisingly, epoxidation of substrates with two alkene functionality takes place selectively on one of alkene functional groups (Table 1, **10j** and **10m**). Epoxidation of 3-methyl-1-(oxiran-2-yl)but-3-en-2-one was selectively take placed on the terminal alkene functional group (Table 1, **10l**), which represent chemoselectivity of the present method toward terminal alkenes than the corresponding conjugate types. Also, the preparation of **10i** and **10k** with high conversion demonstrated that the method is suitable for epoxidation of sterically hindrance olefins (Table 1, **10i** and **10k**). It was observed that internal alkenes afforded higher selectivity than other terminal alkenes (Table 1, **10b**, **10d**, **10e**).

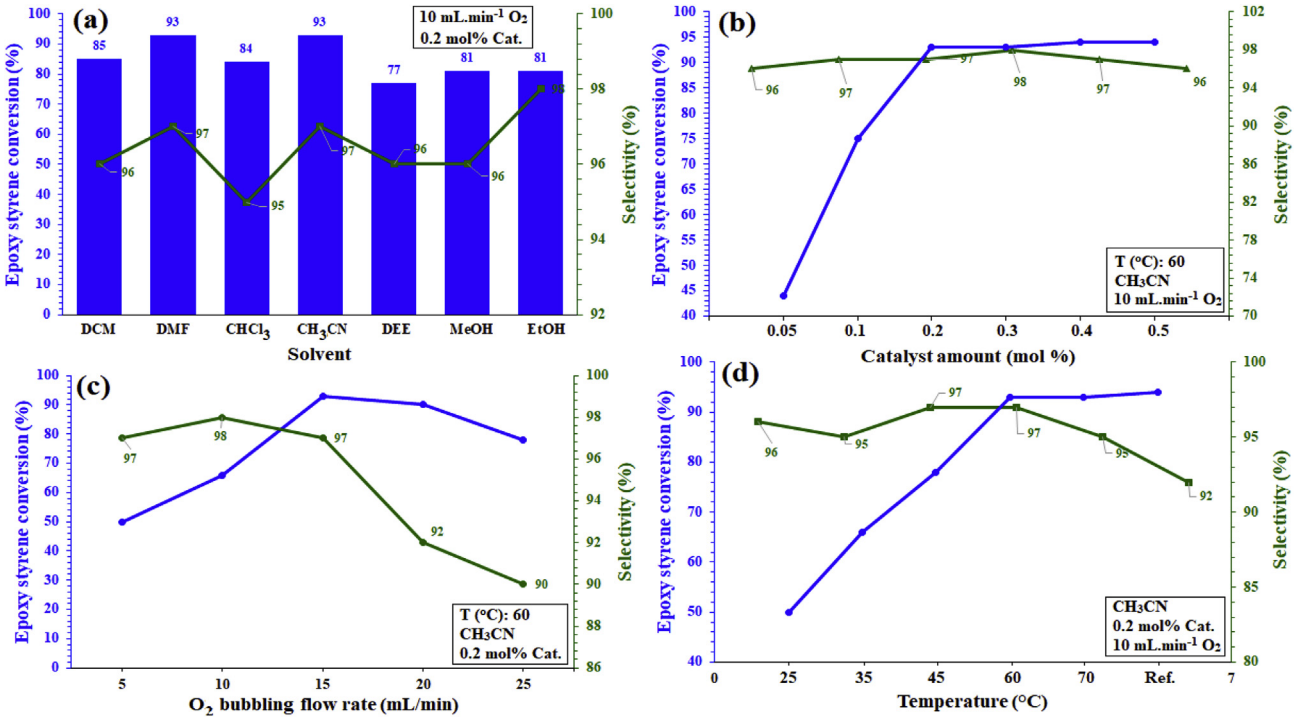

Fig. 5. Screening (a) solvent, (b) catalyst amount, (c) O_2 bubbling flow rate, and (d) temperature on the epoxidation of styrene catalyzed by GO/Fe_3O_4@PAA-Co(II) for 3 h. Green curves demonstrate epoxide selectivity for each study. Conditions: styrene (10.0 mmol), solvent (10 mL). (For interpretation of the references to colour in this figure legend, the reader is referred to the Web version of this article.)

3.3. Control experiments

Some control experiments were conducted to show the exclusive catalytic activity of GO/Fe_3O_4@PAA-Co(II). For this goal, PAA-Co(II) complex, graphene oxide, Fe_3O_4, and $Co(OAc)_2$ were used as catalyst in epoxidation reaction of styrene (10.0 mmol) in CH_3CN in the presence of molecular O_2 (15 mL/min) at 60 °C for 3 h. All the control experiments were conducted under the same conditions. Table 2 shows the corresponding results. GO and Fe_3O_4 afforded inconsiderable efficiency for styrene epoxidation. Also, the selectivity was completely loss for them (Table 2).

$Co(OAc)_2$ provides a moderate efficiency and selectivity (Table 2). Coordination of cobalt into PAA provides only 77% conversion with low selectivity (88%). In this regard, given the presence of free Fe_3O_4 NPs on GO surface in the catalyst, a synergetic effect arising from Fe_3O_4, Co and PAA-Co complex immobilized on GO could be considered. There is not any detectable product in the absence of any catalyst. The results illustrated the advantage and superiority of the support and the designed structure on the catalytic behavior over all applied reagents, which selectively conduct the epoxidation of alkene.

3.4. Mechanism studies

According our observations and other researchers' work [1,30–32], a plausible mechanism was suggested for the epoxidation of olefins with molecular oxygen catalyzed by GO/Fe_3O_4@PAA-Co(II). The suggested mechanism is illustrated in Scheme 4. In first, Co-superoxo active radicals were generated by interaction of the catalyst with O_2 (Scheme 4, Int. I). This was proved by taking XPS analysis of the mixture *in situ*, which the presence of both Co(II) and Co(III) was detected to the mixture (Fig. 6A). Styrene is added to this Co-superoxo intermediate through an oxidative addition reaction, which led to the cyclic intermediate II (Scheme 4). A cyclic peroxide radical (Intermediate III) could be formed from intermediate II and the catalyst is regenerated for the next cycle. This peroxide interacts with another styrene molecule to produce the desired epoxide product. However, the active peroxide may be decomposed to form aldehyde and formaldehyde by-products (Scheme 4), that is not completely consistent with the observed high selectivity in this work for all substrates. Another rote is possible *via* the collapse of II (Scheme 4, bold arrow), which led to a Co-oxo radical (Int. IV) and a desired epoxide molecule, based on the previously reported mechanisms [33,34]. Intermediate IV could be also interacting with another styrene molecule to form epoxide product. Given that high selectivity observed for the substrates, this rote seems to be more probable. However, the formation of epoxide could be takes place through each routes and or a mixture of them. It worth noted that the Co(II) species are only species in the mixture in end of the reaction according to XPS analysis of the recovered catalyst after reaction completion (Fig. 6A–b), which corroborates that the highly active plausible intermediates III and IV are consumed and/or decomposed during reaction.

To support of the suggested radical mechanism, in another control experiment, hydroquinone as a strong and efficient radical scavenger was added to the reaction mixture of styrene at beginning ($t = 0$) as well as 1.5 h of the reaction. Progress of the reactions were monitored every 30 min and the results were gathered in Fig. 6B. As shown in Fig. 6B, the reaction is stopped immediately after addition of hydroquinone. Furthermore, addition of hydroquinone at start of the reaction, almost suppress the reaction progress. These results completely confirm that the epoxidation reaction of olefins catalyzed by GO/Fe_3O_4@PAA-Co(II) accomplished by active radical species as shown in Scheme 4.

The magnetic nanocatalyst **8** could be easily recovered from the mixture and reused for the subsequent reactions without any

Table 1
Epoxidation of alkenes by GO/Fe_3O_4@PAA-Co(II)[a].

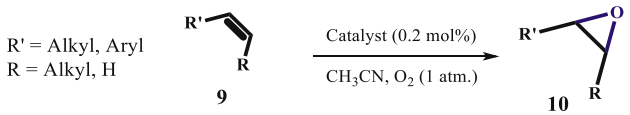

Entry	Product 10		Time (h)	Conversion (%)[b]	Yield (%)[c]	Epoxide selectivity (%)[b]	TOF (h^{-1})[d]
1		**10a**	3	93	88	97	155
2		**10b**	3.5	96	92	97	137
3		**10c**	2.2	94	90	95	213
4		**10d**	2.5	96	93	98	192
5		**10e**	1	99	96	99	495
6		**10f**	8	96	90	95	60
7	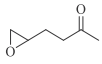	**10g**	1	95	93	99	475
8	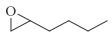	**10h**	7.5	98	94	79	65
9	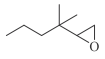	**10i**	24	92	86	86	19
10	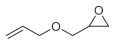	**10j**	1	96	93	80	480
11		**10k**	9	94	82	85	52
12	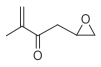	**10l**	45 min	92	88	86	613
13	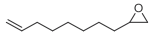	**10m**	1	92	90	84	460

[a] Reaction conditions: alkene (10 mmol), catalyst 8 (50 mg, 0.2 mol%), 60 °C, CH_3CN (10 mL), O_2 (~1 atm. bubbling 15 mL/min), time.
[b] Isolated yield.
[c] GC analysis; using an internal standard technique (Anisole) and is based on alkenes.
[d] Based on conversion.

Table 2
The conversions and selectivities of styrene epoxidation catalyzed by PAA-Co(II) complex, CO, Fe_3O_4, and $Co(OAc)_2$ along with blank experiment.

Catalyst	PAA-Co(II) complex[a]	GO	Fe_3O_4[b]	$Co(OAc)_2$	Blank
Conversion (%)	77	8	38	62	Trace
Selectivity (%)	88	35	57	75	–

[a] PAA-Co(II) complex was prepared by addition of $CoCl_2.6H_2O$ (10 mg) to 1.0 g of PAA in 25 mL ethanol at reflux conditions. The reaction was stirred for 3 h, then the complex filtered, washed and dried at room temperature.
[b] Fe_3O_4 was prepared according to a previously reported procedure [29].

significant reactivity loss (Fig. 7a). The recyclability of the catalyst was investigated for 6 consecutive runs and as a result, didn't found any significant drop in selectivity, epoxide efficiency and catalyst yield. In addition, a small metal leaching was detected in each run that was negligible. The results clearly demonstrate the stability and durability of the catalyst during the reaction. To prove this, the recovered catalyst after 6th run was characterized by some techniques. VSM analysis of the recovered catalyst demonstrated a similar magnetic behavior as same as the corresponding fresh catalyst. There is not any decrease in saturation magnetization. The results were also confirmed the absence of any magnetite leaching from the catalyst surface. Furthermore, the FE-SEM and TEM images from the recovered catalyst revealed that the catalyst preserves its morphology and distribution during several recycling.

It is well known that some catalytic reactions would anyway take place even if an actual catalytic species is leached off from their material [35,36]. Although, a negligible metal leaching was found for the catalyst, to gain more insight into heterogeneous nature of the catalyst, hot filtration test was applied on the model reaction. The catalyst was magnetically removed *in situ* from the epoxidation reaction of styrene in CH_3CN in the presence of molecular oxygen (15 mL/min bubbling) after 1 h of the reaction mixture (44% epoxy styrene conversion). Reaction progress was monitored every 15 min by GC instrument. Didn't observe any significant progress in epoxidation, which the conversion reached to 46% after 3 h. These results are in agreement with leaching studies and confirm that the

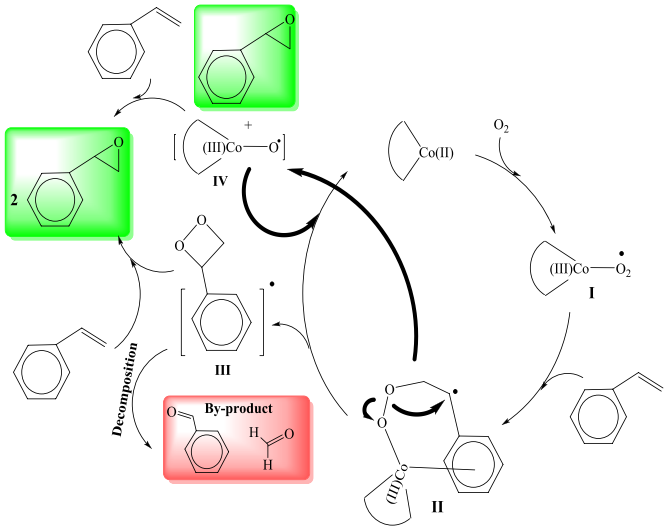

Scheme 4. A plausible reaction mechanism for catalytic epoxidation of olefins using GO/Fe_3O_4@PAA-Co(II)

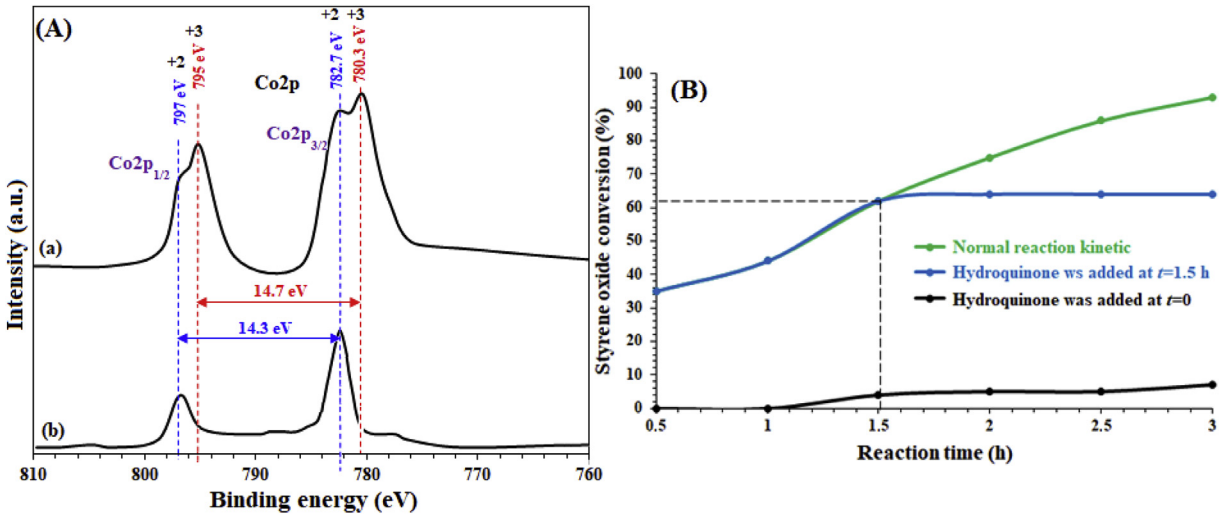

Fig. 6. . (A) (a) *In situ* normalized high-resolution XPS spectrum of the epoxidation reaction mixture of styrene catalyzed by the GO/Fe_3O_4@PAA-Co(II) and (b) XPS spectrum of the recovered catalyst (first cycle). (B) Reaction kinetics (green curve) and effect of hydroquinone on reaction progress at beginning (black curve) and at 62% conversion (blue curve) for the epoxidation reaction of styrene.

catalyst completely act heterogeneously during the reaction.

3.5. Scalability of the method

To investigate the potential of the process for larger scales, the epoxidation reaction of styrene was selected as a model reaction. The reaction was performed under the obtained premium conditions with 200, 500, and 700 mmol of styrene. As presented in Table 3, the results clearly demonstrated the direct scalability of the process, which didn't found any considerable loss in efficiency in term of time, conversion or selectivity even at large quantities (Table 3). However, a reasonable insignificant loss in conversion was observed as the amount of styrene rises; nevertheless, the selectivity was independent than the scale and remained constant thoroughly.

4. Conclusion

In conclusion, a novel synthetic poly α-amino acid-Co(II) complex was immobilized on magnetite graphene oxide (GO/Fe_3O_4@-PAA Co(II)) and used as an efficient nanocatalyst for selective epoxidation of olefins. A wide variety of olefins were subjected to epoxidation using the catalyst, which high to excellent conversions and selectivities were achieved for all of them. The catalyst has a mean size of about 30 nm (from FE-SEM, DLS and TEM analyses) with saturation magnetization of 32 emu. g^{-1} (from VSM analysis) containing 0.2 mol%Co^{2+} (from ICP and XPS analyses). Further characterization of the nanocatalyst was obtained from FTIR, TGA,

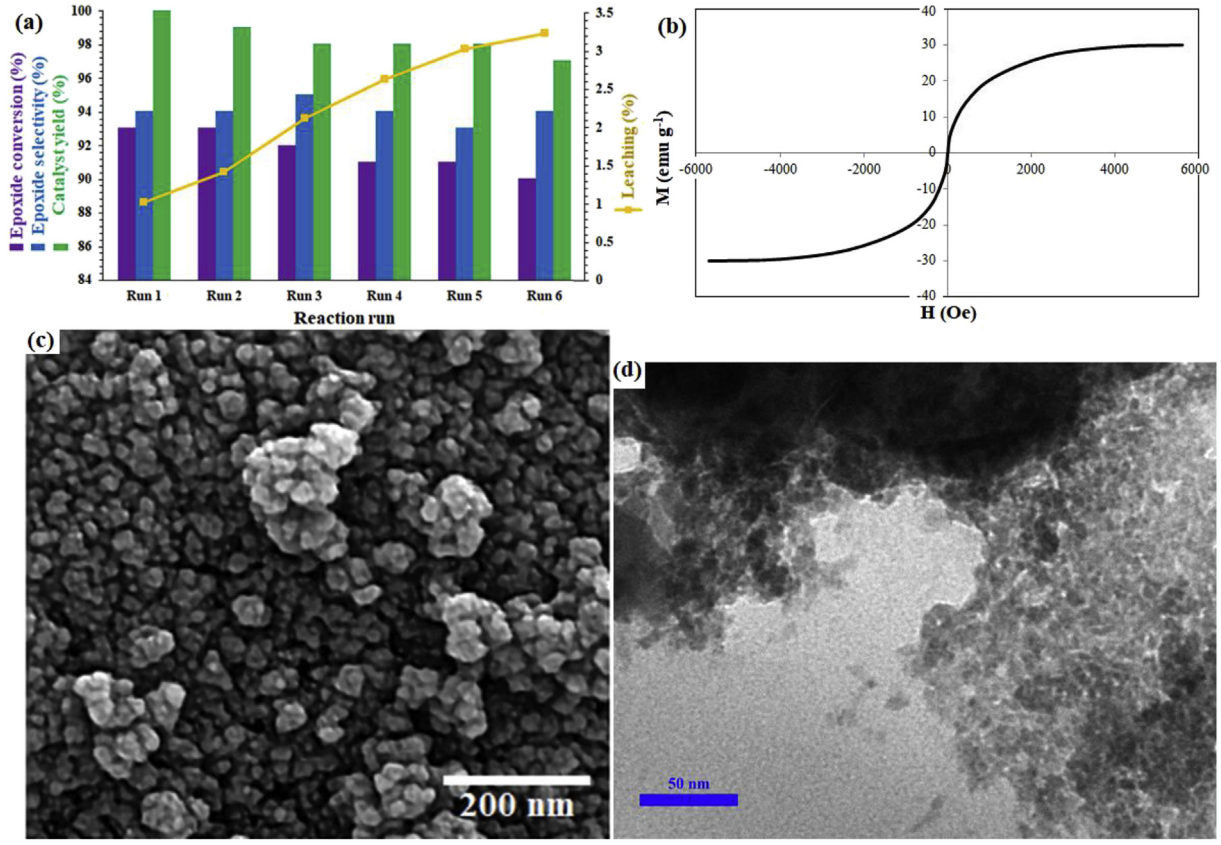

Fig. 7. (A) Recycling of GO/Fe_3O_4@PAA-Co for the oxidation reaction of styrene in CH_3CN at 60 °C in the presence of molecular O_2. (B) VSM curve, (C) FE-SEM, and (D) TEM analysis of the recovered catalyst after 6th run.

Table 3
Gram scale production of epoxy styrene using GO/Fe_3O_4@PAA-Co[a]

Entry	mmol of styrene	Time (h)	Conversion (%)[b]	Selectivity (%)
1	200	3	90	97
2	500	3	88	97
3	700	3	86	95

[a] The reactions were performed in a 1 L round bottom flask and the reactions were mechanically stirred. All experiments were performed in the presence of 15 mL min^{-1} O_2 bubbling (~1 atm.) at 60 °C. For each entry, the amounts of CH_3CN and catalyst **8** were proportional to the amount of styrene (see "General procedure for catalytic epoxidation of olefins by GO/Fe_3O_4@PAA-Co(II)").
[b] GC yield.

EDX, and XRD analyses. Free coreductant, gram scale, mild reaction conditions (CH_3CN, 60 °C), fast performance, selectivity toward epoxide product, durability (insignificant activity loss during six consecutive recycling), thermal stability, magnetically recoverable, and high efficiency epoxide products were some of the advantages of the present protocol, which make it suitable alternative method for the epoxidation program. Furthermore, direct scalability for the process in large quantities was found that is applicable for industrial goals.

Conflicts of interest

There are no conflicts to declare.

Acknowledgment

Authors gratefully acknowledge the financial support of this work by the Research Council of University of Birjand. We also thank Roxana Nayerlou for her critical reading and comment on the manuscript.

Appendix A. Supplementary data

Supplementary data to this article can be found online at https://doi.org/10.1016/j.jorganchem.2019.05.030.

References

[1] M. Kazemnejadi, A. Shakeri, M. Nikookar, M. Mohammadi, M. Esmaeilpour, Res. Chem. Intermed. 43 (2017) 6889–6910.
[2] S.H. Lee, L. Xu, B.K. Park, Y.V. Mironov, S.H. Kim, Y.J. Song, S.J. Kim, Chem. Eur J. 16 (2010) 4678–4685.
[3] D. Swern, Org. React. 7 (2004) 378–434.
[4] P.S. Teo, H.N. Lim, N.M. Huang, C.H. Chia, I. Harrison, Ceram. Int. 38 (2012) 6411–6416.
[5] M. Keshavarz, A. Zarei Ahmady, L. Vaccaro, M. Kardani, Molecules 23 (2018) 330.
[6] S. Tian, Q. Fu, W. Chen, Q. Feng, Z. Chen, J. Zhang, W.C. Cheong, R. Yu, L. Gu, J. Dong, J. Luo, Nat. Commun. 9 (2018) 2353.
[7] C. Weerakkody, S. Biswas, W. Song, J. He, N. Wasalathanthri, S. Dissanayake, D.A. Kriz, B. Dutta, S.L. Suib, Appl. Catal., B 221 (2018) 681–690.
[8] D.T. Bregante, A.M. Johnson, A.Y. Patel, E.Z. Ayla, M.J. Cordon, B.C. Bukowski, J. Greeley, R. Gounder, D.W. Flaherty, J. Am. Chem. Soc. 141 (2019) 7302–7319.
[9] D. Ghosh, B. Febriansyah, D. Gupta, L.K.S. Ng, S. Xi, Y. Du, T. Baikie, Z. Dong, H.S. Soo, ACS Nano 12 (2018) 5903–5912.
[10] R. Egekenze, Y. Gultneh, R. Butcher, Polyhedron 144 (2018) 198–209.
[11] I. Bernar, F.P. Rutjes, J.A. Elemans, R.J. Nolte, Catalysts 9 (2019) 195.
[12] S. Goswami, S. Singha, R. Saha, A.S. Roy, M. Islam, S. Kumar, Inorg. Chim. Acta 486 (2019) 352–360.
[13] M. Vasconcellos-Dias, J. Marreiros, R. Sales, V. Félix, P. Brandão, C.D. Nunes, M.J. Calhorda, Molecules 24 (2019) 578.
[14] A. Nasrallah, G. Grelier, M.I. Lapuh, F.J. Duran, B. Darses, P. Dauban, Eur. J. Org.

Chem. (2018) 5836–5842.
[15] J. Jiang, K. Ma, Y. Zheng, S. Cai, R. Li, J. Ma, Appl. Clay Sci. 45 (2009) 117–122.
[16] S. Ghiami, M.A. Nasseri, A. Allahresani, M. Kazemnejadi, React. Kinet. Mech. Catal. 126 (2019) 383–398.
[17] M. Kazemnejadi, S.A. Alavi, Z. Rezazadeh, M.A. Nasseri, A. Allahresani, M. Esmaeilpour, J. Mol. Struct. 1186 (2019) 230–249.
[18] X. Yang, X. Zhang, Y. Ma, Y. Huang, Y. Wang, Y. Chen, J. Mater. Chem. 19 (2009) 2710–2714.
[19] R. Dalpozzo, Green Chem. 17 (2015) 3671–3686.
[20] M. Kazemnejadi, A. Shakeri, M. Nikookar, R. Shademani, M. Mohammadi, Royal Soc. Open Sci. 5 (2018) 171541.
[21] X.H. Zhang, R.J. Wei, Y.Y. Zhang, B.Y. Du, Z.Q. Fan, Macromolecules 48 (2015) 536–544.
[22] W.S. Hummers Jr., R.E. Offeman, J. Am. Chem. Soc. 80 (1958), 1339-1339.
[23] X. Sun, Z. Liu, K. Welsher, J.T. Robinson, A. Goodwin, S. Zaric, H. Dai, Nano Res. 1 (2008) 203–212.
[24] J. Shen, Y. Hu, M. Shi, N. Li, H. Ma, M. Ye, J. Phys. Chem. C 114 (2010) 1498–1503.
[25] Y.L. Dong, H.G. Zhang, Z.U. Rahman, L. Su, X.J. Chen, J. Hu, X.G. Chen, Nanoscale 4 (2012) 3969–3976.
[26] P. Bilalis, L.A. Tziveleka, S. Varlas, H. Iatrou, Polym. Chem. 7 (2016) 1475–1485.
[27] H. Tourani, M.R. Naimi-Jamal, M.G. Dekamin, Chemistry 3 (2018) 8332–8337.
[28] M. Kazemnejadi, S.A. Alavi, Z. Rezazadeh, M.A. Nasseri, A. Allahresani, M. Esmaeilpour, Green Chem. 21 (2019) 1718–1734.
[29] R. Sardarian, M. Kazemnejadi, M. Esmaeilpour, Dalton Trans. 48 (2019) 3132–3145.
[30] M.J. Beier, W. Kleist, M.T. Wharmby, R. Kissner, B. Kimmerle, P.A. Wright, J.D. Grunwaldt, A. Baiker, Chem. Eur J. 18 (2012) 887–898.
[31] D. Saha, T. Maity, R. Bera, S. Koner, Polyhedron 56 (2013) 230–236.
[32] P. Buranaprasertsuk, Y. Tangsakol, W. Chavasiri, Catal. Commun. 8 (2007) 310–314.
[33] Y.L. Hu, Y.W. Liu, D.J. Li, J. Iran. Chem. Soc. 12 (2015) 2179–2184.
[34] W. Nam, H.J. Kim, S.H. Kim, R.Y. Ho, J.S. Valentine, Inorg. Chem. 35 (1996) 1045–1049.
[35] M. Kazemnejadi, A. Shakeri, M. Mohammadi, M. Tabefam, J. Iran. Chem. Soc. 14 (2017) 1917–1933.
[36] M. Kazemnejadi, M. Nikookar, M. Mohammadi, A. Shakeri, M. Esmaeilpour, J. Colloid Interface Sci. 527 (2018) 298–314.